Journal of Materials Science and Chemical Engineering, 2026, 14(6), 1-11
https://www.scirp.org/journal/msce
ISSN Online: 2327-6053
ISSN Print: 2327-6045

Investigation Insights into Thermoelectric Materials of Ni-Based Heusler Alloys: First-Principles Calculations

Zhengxu Li[1], Yaping Li[2,3], Sujun Guan[2,3*], Lijun Wang[4], Taishu Chishima[1], Hiroyuki Yoshida[5], Ryosuke Yamagata[1], Takaomi Itoi[1], Yun Lu[1,4*]

[1]College of Mechanical Engineering & Graduate School, Chiba University, Chiba, Japan
[2]School of Physics and Advanced Energy, Henan University of Technology, Zhengzhou, China
[3]R&D Center for Advanced Energy Materials, Henan University of Technology, Zhengzhou, China
[4]School of New Energy Engineering, Chengdu Technological University, Yibin, China
[5]Chiba Industrial Technology Research Institute, Chiba, Japan
Email: *guansujun@haut.edu.com, *luyun@faculty.chiba-u.jp

How to cite this paper: Li, Z.X., Li, Y.P., Guan, S.J., Wang, L.J., Chishima, T., Yoshida, H., Yamagata, R., Itoi, T. and Lu, Y. (2026) Investigation Insights into Thermoelectric Materials of Ni-Based Heusler Alloys: First-Principles Calculations. *Journal of Materials Science and Chemical Engineering*, **14**, 1-11.
https://doi.org/10.4236/msce.2026.146001

Received: March 24, 2026
Accepted: June 20, 2026
Published: June 23, 2026

Abstract

Ni-based Heusler alloys, as intermetallic compounds and high-temperature alloys, possess superior properties, including high-temperature oxidation resistance, corrosion resistance, and excellent advantages for application as thermoelectric materials. Herein, a screening study of Ni-based Heusler alloys was carried out using first-principles calculations combined with the BoltzTraP software, focusing on investigating their electronic structure and density of states (DOS) with the aim of achieving a high thermoelectromotive force. Studies on the Heusler alloys have confirmed that their valence electron density is equal to 6, accompanied by a sharp DOS mutation near the Fermi level. Based on Mott theory, this gives rise to a large Seebeck coefficient, enabling a breakthrough in the longstanding limitation of the low Seebeck coefficient of conventional Heusler alloys used as thermoelectric materials.

Keywords

Ni Alloy System, Heusler Alloy, First-Principles Calculation, DOS, Band Construction, Thermoelectric Property

1. Introduction

Heusler alloys are typically classified into two categories: full-Heusler alloys with a stoichiometry of X_2YZ (X, Y = transition metal elements; Z = sp-group elements) and half-Heusler alloys with XYZ. Ni-Ti-Al-based Heusler alloys are typical high-

temperature structural materials, exhibiting excellent high-temperature corrosion resistance, oxidation resistance, and mechanical strength [1] [2]. For Heusler alloys applied as thermoelectric materials, material design and performance enhancement strategies based on their unique electronic structures have been well established. For instance, Fe_2VAl, a well-known full-Heusler thermoelectric alloy, features a pseudogap in its density of states (DOS) profile [3] [4] with low DOS at the Fermi level (E_F) and an abrupt variation in DOS near E_F. Notably, ZrNiSn, a representative half-Heusler alloy [5], also shows a low DOS at E_F and an abrupt DOS change in the vicinity of E_F, analogous to full-Heusler alloys, despite its extremely narrow band gap. According to Mott's theory [6] [7], optimizing the E_F within the pseudogap can enhance the thermoelectromotive force (Seebeck coefficient) and reduce electrical resistivity, laying a theoretical foundation for thermoelectric material design.

To date, high power factors exceeding those of conventional thermoelectric materials (Bi_2Te_3 and PbTe) [8] have been achieved via material design and fabrication strategies such as non-stoichiometric composition engineering and heavy element substitution [9] [10]. It has been reported that a figure of merit (ZT) > 1 is attainable by optimizing carrier density, reducing thermal conductivity through nanostructure precipitation, and elemental substitution with Hf, Co, Zr, Nb, etc. [11]. However, for practical application and industrialization, critical challenges remain, including further thermal conductivity reduction and the avoidance of heavy element usage, limitations that motivate the exploration of alternative Heusler alloy systems.

On the other hand, thermoelectric materials have garnered significant attention owing to their ability to realize the mutual conversion of thermal and electrical energy, enabling the efficient utilization of waste heat. However, the thermoelectric materials currently considered promising for waste heat recovery applications rely on toxic and costly elements, which hinder their large-scale deployment. To address this issue, Heusler alloy-based thermoelectric materials, fabricable from common metallic elements, have emerged as a promising alternative. Notably, certain Heusler alloys exhibit a low DOS at the Fermi level coupled with an abrupt DOS variation in its vicinity [3] [4], a characteristic that can be harnessed to enhance thermoelectric performance.

Heretofore, we have focused on Ni-based Heusler alloys, which possess excellent corrosion and heat resistance, as a replacement for Fe_2VAl (the highest-performance Heusler alloy thermoelectric material reported to date), and successfully synthesized Ni_2TiAl in our previous work [12]. Nevertheless, the thermoelectric performance of Ni_2TiAl remains far from practical application, necessitating a re-evaluation of its composition. In recent years, an increasing number of researchers have focused on Ni_2TiAl Heusler alloys for thermoelectric applications [13]-[16], highlighting the relevance of further investigating this alloy system.

To address the aforementioned gaps and build on existing research, this study employs first-principles calculations to analyze the electronic structure and DOS

of Ni-based Heusler alloys, with the aim of achieving high thermoelectromotive force. Specifically, the objective is to identify favorable compositions of Ni-based Heusler alloys for thermoelectric applications by elucidating the relationship between their electronic structures and thermoelectric potential.

Accordingly, the electronic structure of Ni-based Heusler alloys was analyzed via first-principles calculations, with a focus on compositions featuring low DOS at the Fermi level (E_F) and abrupt DOS variations near E_F, which are key characteristics for enhanced thermoelectric performance. Thermoelectric performance was further predicted using the BoltzTraP method [17] [18]. Through these approaches, we investigated the composition of promising Ni-based system Heusler alloy thermoelectric materials and explored strategies for their performance enhancement.

2. Methods

Previous studies on the full-Heusler and half-Heusler alloy, both of which are regarded as promising thermoelectric materials [3]-[5]. A pseudogap forms near the Fermi level (E_F) when these alloys satisfy specific total valence electron count (VEC) rules: full-Heusler alloys with a stoichiometry of X_2YZ (composed of 4 atoms) require a total VEC of 24, and half-Heusler alloys with a stoichiometry of XYZ (composed of 3 atoms) require a total VEC of 18. Notably, both rules correspond to an average of 6 VEC per atom (24 VEC ÷ 4 atoms = 6 VEC/atom for full-Heusler; 18 VEC ÷ 3 atoms = 6 VEC/atom for half-Heusler). Building on this established rule, we proposed several Ni-based Heusler (full-Heusler: Ni_2TiAl, $(Ni_{0.5}Mn_{0.5})_2TiAl$, $(Co_{0.5}Fe_{0.5})_2ScAl$) and half-Heusler (NiVAl, NiVIn) compositions with a target VEC of 6 per atom average, and systematically investigated their electronic properties and thermoelectric performance. This 6 per atom VEC criterion was selected because it ensures the formation of a pseudogap near E_F, which is critical for achieving a large Seebeck coefficient and high thermoelectric performance, as confirmed by Mott's theory—specifically, the pseudogap leads to a low DOS at E_F and a steep DOS slope near E_F, both of which are beneficial for enhancing the Seebeck coefficient.

Density Functional Theory is an electronic structure calculation method based on the Hohenberg-Kohn (HK) theorems, which state that physical properties such as the total energy of an electron system can be calculated solely from the electron density [19]. Using first-principles density functional theory (DFT) calculations, we analyzed the DOS near the Fermi level, its evolution across different compositions, and the resulting band structures. The Generalized Gradient Approximation (GGA) variant adopted in this work was Perdew-Burke-Ernzerhof (PBE) [20], which incorporates the effect of electron density gradients into the Local Density Approximation (LDA). PBE was chosen for its balance of accuracy and computational efficiency in predicting the electronic structures of transition metal Heusler alloys. LDA treats the charge density as a uniform electron gas; however, the actual charge density distribution is non-uniform, and PBE-GGA improves

the calculation accuracy of LDA by introducing the gradient effect of charge density.

Computational details are specified as follows: Pseudopotentials were ultrasoft pseudopotentials with a plane-wave energy cutoff of 680 eV, and the wavefunction solver was set to mddavidsom → rmm3 for self-consistent field (SCF) calculations. Spin treatment was spin-unpolarized, as preliminary spin-polarized calculations showed no significant difference in electronic structure or thermoelectric properties for the selected Ni-based Heusler alloys. Structural relaxation was performed using the conjugate gradient method, optimizing lattice constants and atomic positions until the maximum force on each atom was less than 5.0×10^{-4} Hartree and the total energy convergence was less than 1.0×10^{-9} Hartree. The general calculation parameters are listed in Table 1.

Table 1. The calculation parameters.

Parameter	Value
Plane-wave energy cutoff	680 eV
Wavefunction solver	mddavidsom → rmm3
Convergence criterion (SCF)	2.7×10^{-9} Hartree (two self-consistent cycles)
K-point mesh	3 × 3 × 3
Auxiliary energy cutoff	25 Hartree
Combined wavefunction solver	mdd + rmm3
Energy convergence threshold	1.0×10^{-9} Hartree
Force convergence threshold	5.0×10^{-4} Hartree

First-principles calculations were conducted using the PHASE/0 software package (ASMS Co., Ltd.) [18]. Crystal structures were obtained through two approaches: 1) Direct retrieval from the inorganic material database AtomWork [21]. Ni_2TiAl (full-Heusler), NiVAl (half-Heusler), Fe_2VAl (benchmark full-Heusler), and ZrNiSn (benchmark half-Heusler) crystal structures were downloaded directly from the database, as their structural data were fully available. 2) Elemental substitution for materials without available structural data: $(Ni_{0.5}Mn_{0.5})_2TiAl$, $(Co_{0.5}Fe_{0.5})_2ScAl$ (full-Heusler), and NiVIn (half-Heusler) were constructed by elemental substitution based on the Ni_2TiAl (for full-Heusler) and NiVAl (for half-Heusler) crystal structures retrieved from AtomWork. For substituted structures, lattice constants and atomic positions were optimized via the conjugate gradient method, and structural stability was verified by calculating the phonon dispersion curves—all substituted structures exhibited no imaginary frequencies, confirming their thermodynamic stability. All obtained crystal structures were adopted for subsequent calculations using the PHASE/0 software, based on the Heusler structure [22] depicted in Figure 1.

The Hohenberg-Kohn (HK) theorems consist of two fundamental theorems for non-degenerate ground-state N-electron systems. The first theorem states that, for a given external potential V, the ground-state energy E_G is uniquely determined

by the single-electron density $\rho(r)$. The second theorem states that the ground-state energy functional $E_G[\rho]$ attains its minimum value when the N-normalized trial electron density $\rho'(r)$ coincides with the true ground-state electron density $\rho(r)$.

The HK theorems demonstrate that the Hamiltonian of an electronic system can be expressed solely in terms of the electron density. It is also proven that any Hamiltonian constructed from an N-representable electron density always possesses a solution corresponding to the minimum energy.

$$\left(-\frac{\hbar^2}{2m}\nabla^2 + V_{eff}(r)\right)\psi_i = \varepsilon_i\psi_i \tag{1}$$

The computational formalism established on the basis of the HK theorems is the Kohn-Sham (KS) equation. The KS equation introduces an auxiliary system independent of the real physical system, and seeks the effective potential V_{eff} such that the ground-state electron density of the auxiliary system matches that of the real system. In KS theory, the HK energy functional takes the following form:

$$E = -\frac{\hbar^2}{2m}\int dr\psi_i^*(r)\nabla^2\psi_i(r) + \frac{e^2}{4\pi\varepsilon_0}\iint drdr'\frac{n(r)n(r')}{|r-r'|} + \int drV_{ext}(r)n(r) + E_{XC} \tag{2}$$

where n denotes the ground-state electron density of the auxiliary system, V_{ext}(r) is the external potential of the real system, and E_{XC} is the exchange-correlation energy. Performing the variational treatment of this expression in accordance with the second HK theorem yields the corresponding variational equation.

$$V_{eff}(r) = V_{ext}(r) + \frac{e^2}{4\pi\varepsilon_0}\int dr'\frac{n(r')}{|r-r'|} + \frac{\delta E_{XC}}{\delta n(r)} \tag{3}$$

For practical numerical calculations, an explicit analytical form of E_{XC} is indispensable. Various compositions were investigated by assuming a full-Heusler (X_2YZ) or half-Heusler (XYZ) configuration. Specifically, Ni, Ti, and Al atoms were substituted with target elements (e.g., V and In), with interatomic distances optimized according to relevant literature. For other alloys, structural parameters were retrieved from the Inorganic Materials Database [21] to ensure computational accuracy.

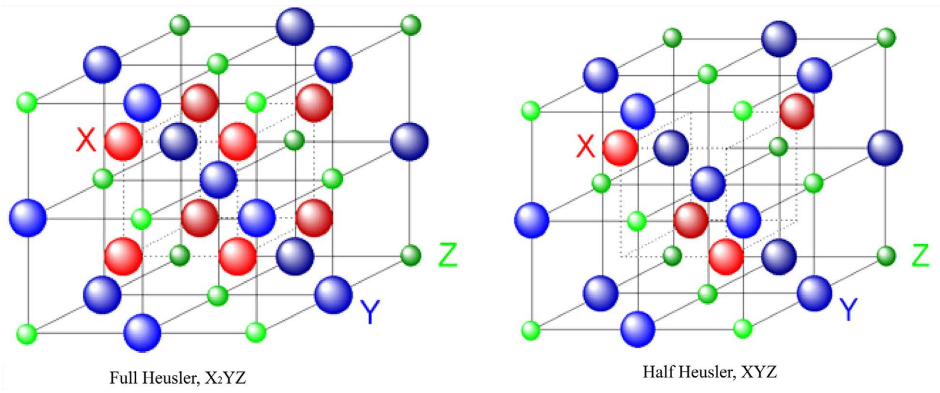

Figure 1. Crystal structure of Heusler alloy.

Regarding the dimensionless ZT, the relaxation time must be assumed, and the phonon thermal conductivity cannot be calculated. We considered the calculated result (Z_eT) as the theoretical upper limit of the thermoelectric performance with such a formula, and studied it. Z_eT is a value normalized solely by the electronic thermal conductivity, unlike ZT, which is usually divided by the sum of carrier heat conduction and phonon heat conduction. This formula makes it possible to calculate the thermoelectric performance without including the unknown constant of relaxation time.

This program calculates transport functions using the Boltzmann transport equation, based on the DOS of NiTiAl, NiVAl, $(Co_{0.5}Fe_{0.5})_2$TiAl, and $(Ni_{0.5}Fe_{0.5})_2$ScAl obtained from first-principles calculations. The Seebeck coefficient, electrical conductivity, and electronic thermal conductivity were computed via the BoltzTraP code [23]. For these calculations, a constant relaxation time (τ) of 0.1×10^{-14} s was initially assumed.

Regarding the dimensionless Z_eT, a specific relaxation time must typically be assumed, and the lattice (phonon) thermal conductivity (κ_L) remains inaccessible through this method. Consequently, we adopted the Z_eT to represent the theoretical upper limit of thermoelectric performance. Unlike the conventional Z_eT, which is divided by the sum of electronic (κ_e) and lattice (κ_L) thermal conductivities, Z_eT is defined solely by the electronic contribution. This formulation allows for the evaluation of thermoelectric potential without the uncertainty introduced by the unknown relaxation time constant, as τ cancels out in the ratio of σ/κ_e according to the Wiedemann-Franz law.

3. Results

3.1. First-Principles Density of States Calculations

Figure 2 shows the band structure and DOS of the Ni-M-Al system, Half Heusler and $(A_{0.5}B_{0.5})_2$-M-Al system Full Heusler alloys. The Half Heusler alloys NiTiAl, NiVAl, $(Co_{0.5}Fe_{0.5})_2$TiAl, and $(Ni_{0.5}Fe_{0.5})_2$ScAl. The computational results reveal the emergence of a pseudogap near the E_F in all samples, which is consistent with the VEC = 6 per atom design rule. Specifically, the band structure of NiVAl (half-Heusler) exhibits a distinct energy gap directly at the Fermi level (0.21 eV), while NiVIn (half-Heusler) shows a pseudogap with a minimum DOS of 0.06 states/eV/atom near E_F. For full-Heusler alloys, $(Ni_{0.5}Mn_{0.5})_2$TiAl and $(Co_{0.5}Fe_{0.5})_2$ScAl exhibit shallower pseudogaps with minimum DOS of 0.12 and 0.15 states/eV/atom, respectively, while Ni_2TiAl shows a broader pseudogap with a minimum DOS of 0.10 states/eV/atom. The benchmarks Fe_2VAl and ZrNiSn exhibit pseudogaps with minimum DOS of 0.08 and 0.07 states/eV/atom, respectively, consistent with published data [3] [5]. This electronic structure is closely attributed to the average VEC of 6 per atom, confirming the validity of our design criterion. The Seebeck coefficient can be derived using the following expression [24]:

$$S = -\frac{\pi^2}{3}\frac{k_B T}{e}\frac{1}{D(E_F)}\left[\frac{\partial D}{\partial E}\right]_{E=E_F} \tag{4}$$

The Seebeck coefficient is typically enhanced by a low DOS at the Fermi level, D(E_F), coupled with a steep DOS slope in its vicinity. In the case of full-Heusler alloys $(Co_{0.5}Fe_{0.5})_2TiAl$ and $(Ni_{0.5}Fe_{0.5})_2ScAl$, the gap formation is significantly shallower than that of half-Heusler alloys like NiTiAl and NiVAl, with a residual DOS remaining at approximately 0.20 eV. Consequently, the DOS slope near the Fermi level is relatively gentle. Based on these electronic features, it is predicted that these two full-Heusler alloys will exhibit smaller Seebeck coefficients compared to the calculated values for the half-Heusler alloys.

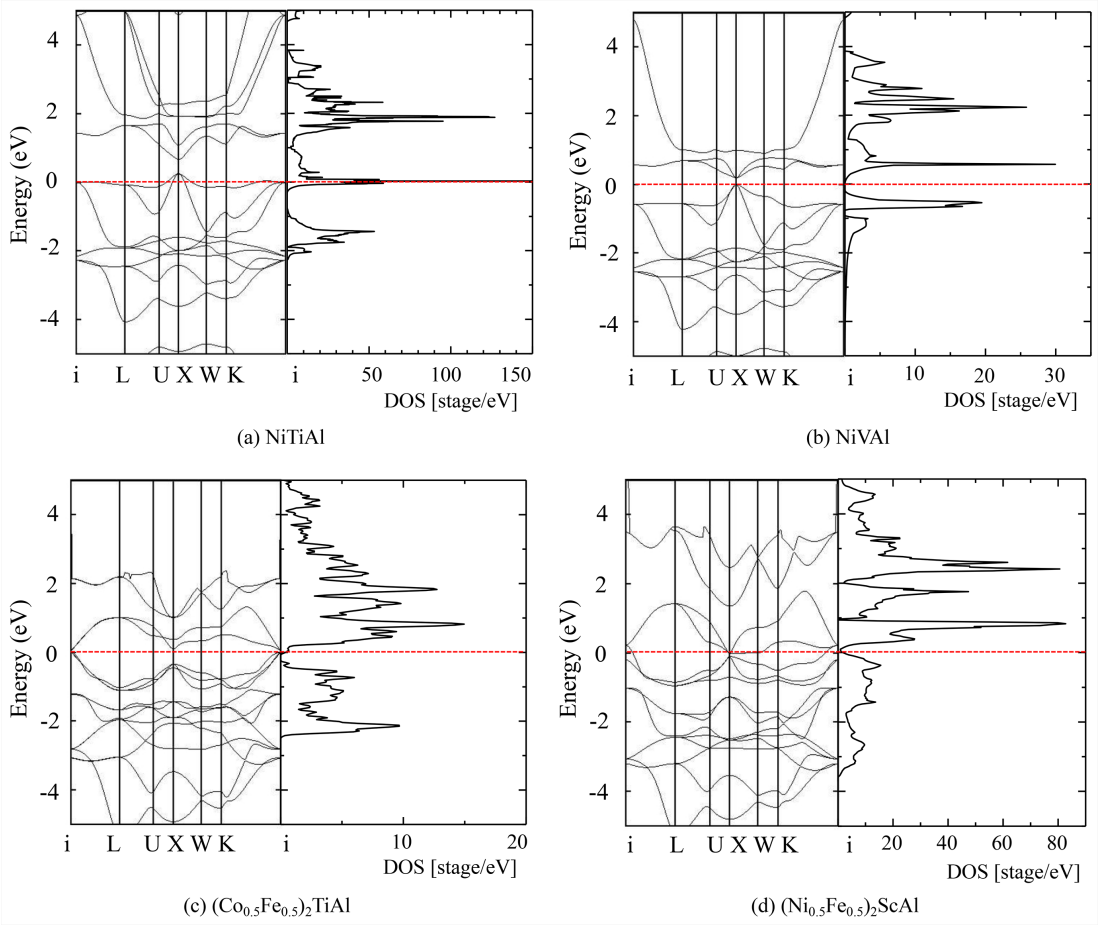

Figure 2. Band structure and DOS of Ni-M-Al system half Heusler and $(A_{0.5}B_{0.5})_2$-M-Al system full Heusler alloys.

3.2. Calculation of Thermoelectric Properties

For this study, Fe_2VAl and ZrNiSn were selected as high-performance benchmarks for full-Heusler and half-Heusler alloys, respectively. Among the full-Heusler alloys, both $(Ni_{0.5}Mn_{0.5})_2TiAl$ and $(Co_{0.5}Fe_{0.5})_2ScAl$ exhibited a transition from n-type to p-type semiconductor behavior at low temperatures, yielding a substantial Seebeck coefficient. **Figure 3** illustrates the Seebeck coefficient (S) and the dimensionless Z_eT for the Heusler and half-Heusler alloys. For this study, we compared Fe_2VAl and NiZrSn, which represent the high-performance benchmarks for their respective structures. Among the Heusler alloys, both $(Ni_{0.5}Mn_{0.5})_2TiAl$ and

$(Co_{0.5}Fe_{0.5})_2ScSi$ exhibited a transition from n-type to p-type semiconductor behavior at low temperatures, yielding a substantial Seebeck coefficient. As a key parameter determining thermoelectric performance, the Seebeck coefficient directly correlates with the dimensionless Z_eT—the magnitude of S is positively associated with Z_eT, as Z_eT is comprehensively determined by S, electrical resistivity (ρ), and thermal conductivity (κ), according to the following relationship:

$$Z_eT = \frac{S^2T}{\rho\kappa} \tag{5}$$

It is evident from the formula that the square of the Seebeck coefficient (S^2) is a dominant factor in enhancing Z_eT: a higher S directly boosts the numerator of the Z_eT equation, thereby improving the overall thermoelectric performance. Consequently, we achieved a higher power factor than the benchmark Fe_2VAl, which was primarily driven by the significant enhancement of the Seebeck coefficient; however, the resulting Z_eT still falls short of the requirements for practical thermoelectric application.

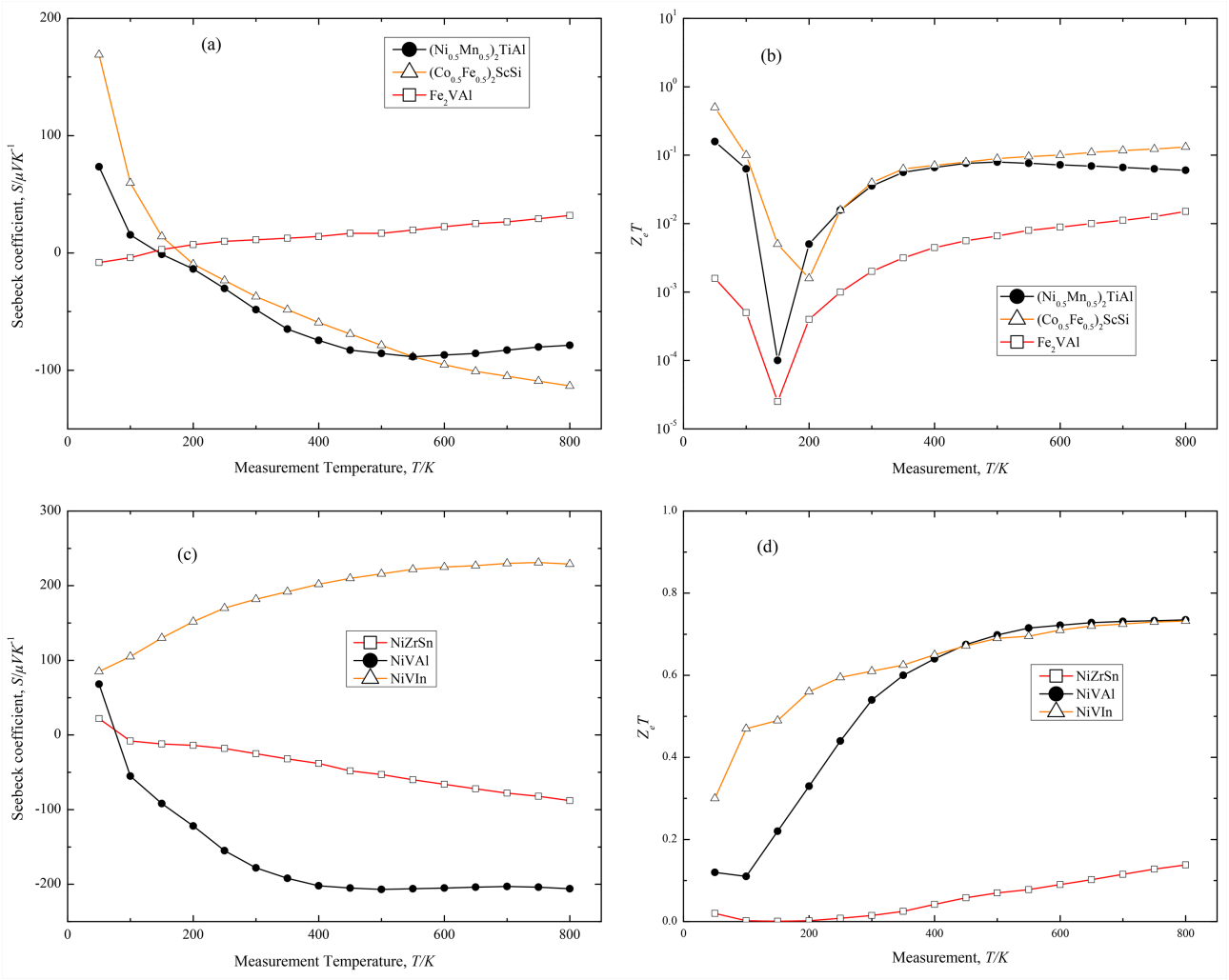

Figure 3. Seebeck coefficient and Z_eT of Heusler and half Heusler alloys.

In full-Heusler alloys, The Seebeck coefficient of $(Ni_{0.5}Mn_{0.5})_2TiAl$ reaches its peak value of −90 μV/K at 550 K, exhibiting n-type semiconductor behavior. For $(Co_{0.5}Fe_{0.5})_2ScSi$, the coefficient is −113 μV/K at 800 K, also indicating n-type conduction. In contrast, Fe_2VAl shows a Seebeck coefficient of approximately 12 μV/K at 300 K, corresponding to p-type semiconductor behavior. NiVAl exhibits a ZeT value of 0.74 at 700 K, which is the highest among all full-Heusler alloys in this study. In half-Heusler alloys, NiVAl typically exhibits n-type semiconducting behavior across the entire temperature range (100 - 900 K), whereas NiVIn functions as a p-type semiconductor across various compositions [25]. Notably, the Seebeck coefficients of both NiVAl and NiVIn surpass those of the benchmark material ZrNiSn, with NiVIn showing the highest peak S (~230 μV/K). Given the direct correlation between S and Z_eT, the elevated Seebeck coefficients of these half-Heusler alloys lay a solid foundation for high Z_eT values. Furthermore, our calculations indicate that NiVIn reaches a Z_eT approaching 0.80 at 800 K, which is higher than that of NiZrSn, confirming its great potential as a promising candidate for thermoelectric applications.

4. Conclusion

We performed first-principles calculations to determine the density of states of selected Ni-based Heusler alloys, which then served as the basis for predicting thermoelectric performance using the BoltzTraP package. A design rule of average VEC = 6 per atom was adopted, which is derived from the established 24-electron full-Heusler and 18-electron half-Heusler rules. This design rule ensures the formation of a pseudogap near E_F, which is an electronic characteristic for enhancing thermoelectric performance by promoting a large Seebeck coefficient. Validation against the benchmark Fe_2VAl confirmed the reliability of our computational workflow, with calculated DOS and Seebeck coefficient consistent with published data. The findings reveal that within the selected Ni-based Heusler alloy family, the calculated Seebeck coefficients for $(Ni_{0.5}Mn_{0.5})_2TiAl$ and $(Co_{0.5}Fe_{0.5})_2ScAl$ both exceeded that of the benchmark Fe_2VAl. Their maximum Z_eT values are substantial but currently remain below the threshold required for commercial applications. However, considering that the performance of Fe_2VAl—a material under intensive contemporary research—can be elevated to practical levels through strategies such as elemental substitution and doping, $(Ni_{0.5}Mn_{0.5})_2TiAl$ and $(Co_{0.5}Fe_{0.5})_2ScAl$ emerge as highly promising candidates for high-performance thermoelectric compositions. For the half-Heusler alloys, NiVAl and NiVIn exhibit superior performance relative to the established benchmark ZrNiSn. Specifically, NiVIn achieves a maximum Z_eT of approximately 0.80 at 800 K, which is close to the practical application threshold. Given these promising theoretical results, they are of great guiding value for conducting experimental fabrication and demonstration.

Authors' Contributions

Conceptualization: Z.L., S.G., and Y.L.; Methodology: Z.L.; Software: Z.L.; Validation: Z.L., L.W., and T.C.; Formal Analysis: Z.L.; Investigation: Z.L.; Resources:

Y.L.; Data Curation: Z.L.; Writing—Original Draft Preparation: Z.L. and Y.L.; Writing—Review and Editing: S.G., Y.L., R.Y., and T.I.; Visualization: H.Y.; Supervision: Y.L.; Project Administration: S.G. and Y.L.; Funding Acquisition: Y.L. All authors have read and agreed to the published version of the manuscript.

Data Availability Statement

The original contributions presented in this study are included in the article. Further inquiries can be directed to the corresponding author.

Conflicts of Interest

The authors declare no conflicts of interest regarding the publication of this paper.

References

[1] Song, X., Li, Y. and Zhang, F. (2014) Microstructure and Mechanical Properties of Nb- and Mo-Modified NiTi-Al-Based Intermetallics Processed by Isothermal Forging. *Materials Science and Engineering*: *A*, **594**, 229-234. https://doi.org/10.1016/j.msea.2013.11.070

[2] Hardy, M.C., Detrois, M., McDevitt, E.T., Argyrakis, C., Saraf, V., Jablonski, P.D., *et al*. (2020) Solving Recent Challenges for Wrought Ni-Base Superalloys. *Metallurgical and Materials Transactions A*, **51**, 2626-2650. https://doi.org/10.1007/s11661-020-05773-6

[3] Nishino, Y. (2011) Development of Thermoelectric Materials Based on Fe_2VAl Heusler Compound for Energy Harvesting Applications. *IOP Conference Series*: *Materials Science and Engineering*, **18**, Article ID: 142001. https://doi.org/10.1088/1757-899x/18/14/142001

[4] Garmroudi, F., Parzer, M., Riss, A., Ruban, A.V., Khmelevskyi, S., Reticcioli, M., *et al*. (2022) Anderson Transition in Stoichiometric Fe_2VAl: High Thermoelectric Performance from Impurity Bands. *Nature Communications*, **13**, Article No. 3599. https://doi.org/10.1038/s41467-022-31159-w

[5] Quinn, R.J. and Bos, J.G. (2021) Advances in Half-Heusler Alloys for Thermoelectric Power Generation. *Materials Advances*, **2**, 6246-6266. https://doi.org/10.1039/d1ma00707f

[6] Izawa, T., Takashima, K., Konabe, S. and Yamamoto, T. (2017) Optimization of Thermoelectric Power Factor and Deviation from Mott's Formula of Edge-Disordered Semiconducting Graphene Nanoribbons. *Synthetic Metals*, **225**, 98-102. https://doi.org/10.1016/j.synthmet.2016.12.023

[7] Mott, N.F. and Harry, J. (1958) The Theory of the Properties of Metals and Alloys. Dover Publications.

[8] Mamur, H., Bhuiyan, M.R.A., Korkmaz, F. and Nil, M. (2018) A Review on Bismuth Telluride (Bi_2Te_3) Nanostructure for Thermoelectric Applications. *Renewable and Sustainable Energy Reviews*, **82**, 4159-4169. https://doi.org/10.1016/j.rser.2017.10.112

[9] Takeuchi, T., Terazawa, Y., Furuta, Y., Yamamoto, A. and Mikami, M. (2013) Effect of Heavy Element Substitution and Off-Stoichiometric Composition on Thermoelectric Properties of Fe_2VAl-Based Heusler Phase. *Journal of Electronic Materials*, **42**, 2084-2090. https://doi.org/10.1007/s11664-013-2532-0

[10] Park, G., Lee, H.S. and Yi, S. (2022) Effects of Annealing on the Microstructure and

Thermoelectric Properties of Half-Heusler Mnisn (M = Ti, Zr, Hf). *Journal of Electronic Materials*, **51**, 3485-3494. https://doi.org/10.1007/s11664-022-09627-2

[11] Kanomata, T. (2011) Heusler Alloys as Functional Materials. Uchida Rokakuho Publishing Co., LTD.

[12] Lu, Y. and Hirohashi, M. (1999) Thermal Behavior during Combustion Synthesis on Intermetallic Compound of Ni-Al System. *Journal of Materials Science Letters*, **18**, 395-398. https://doi.org/10.1023/a:1006636802186

[13] Chen, R., Kang, H., Min, R., Chen, Z., Guo, E., Yang, X., *et al*. (2024) Thermoelectric Properties of Half-Heusler Alloys. *International Materials Reviews*, **69**, 83-106. https://doi.org/10.1177/09506608231225613

[14] Chen, X., Zhang, X., Gao, J., Li, Q., Shao, Z., Lin, H., *et al*. (2021) Computational Search for Better Thermoelectric Performance in Nickel-Based Half-Heusler Compounds. *ACS Omega*, **6**, 18269-18280. https://doi.org/10.1021/acsomega.1c02172

[15] Sharma, R., Gandi, S. and Parne, S.R. (2026) Investigation of Electronic Properties of Novel Half-Heusler Alloys Using Density Functional Theory. *Bulletin of Materials Science*, **49**, Article No. 15. https://doi.org/10.1007/s12034-025-03514-2

[16] Zhang, Y., Peng, G., Li, S., Wu, H., Chen, K., Wang, J., *et al*. (2024) Phase Interface Engineering Enables State-of-the-Art Half-Heusler Thermoelectrics. *Nature Communications*, **15**, Article No. 5978. https://doi.org/10.1038/s41467-024-50371-4

[17] Miyata, M., Ozaki, T., Takeuchi, T., Nishino, S., Inukai, M. and Koyano, M. (2018) High-Throughput Screening of Sulfide Thermoelectric Materials Using Electron Transport Calculations with Openmx and Boltztrap. *Journal of Electronic Materials*, **47**, 3254-3259. https://doi.org/10.1007/s11664-017-6020-9

[18] https://www.asms.co.jp/

[19] Argaman, N. and Makov, G. (2000) Density Functional Theory: An Introduction. *American Journal of Physics*, **68**, 69-79. https://doi.org/10.1119/1.19375

[20] Henderson, T.M., Janesko, B.G. and Scuseria, G.E. (2008) Generalized Gradient Approximation Model Exchange Holes for Range-Separated Hybrids. *The Journal of Chemical Physics*, **128**, Article ID: 194105. https://doi.org/10.1063/1.2921797

[21] Inorganic Material Database: AtomWork. https://crystdb.nims.go.jp

[22] Graf, T., Felser, C. and Parkin, S.S.P. (2011) Simple Rules for the Understanding of Heusler Compounds. *Progress in Solid State Chemistry*, **39**, 1-50. https://doi.org/10.1016/j.progsolidstchem.2011.02.001

[23] Madsen, G.K.H. and Singh, D.J. (2006) BoltzTraP. A Code for Calculating Band-Structure Dependent Quantities. *Computer Physics Communications*, **175**, 67-71. https://doi.org/10.1016/j.cpc.2006.03.007

[24] Tan, G., Zhao, L. and Kanatzidis, M.G. (2016) Rationally Designing High-Performance Bulk Thermoelectric Materials. *Chemical Reviews*, **116**, 12123-12149. https://doi.org/10.1021/acs.chemrev.6b00255

[25] Ohkubo, K., Terada, Y., Takizawa, S., Mohri, T. and Suzuki, T. (1996) Thermal and Electrical Conductivities of Intermetallic Compound Nial with Non-Stoichiometric Composition. *Journal of the Japan Institute of Metals*, **60**, 695-699. https://doi.org/10.2320/jinstmet1952.60.8_695